NONLINEAR ANALYSIS AND IMPROVED DESIGN OF SINGLE-SIDED BONDED PATCH REPAIRS

ADRIANA SANDU, MARIN SANDU, DAN MIHAI CONSTANTINESCU

Abstract. This paper presents a relatively simple and effective procedure to design single-sided adhesively bonded patch repairs in the case of cracked plates in tension. Starting from analytical relations presented in the literature, a more general approach was realized in order to evaluate both the repairs with adherends of constant thickness and the situation when the adherends are tapered in the overlap zone. Nonlinear finite element analyses were made in order to validate the analytical model. The good agreement between the obtained results indicates that analytical solutions are able to put into evidence the geometrical nonlinearity of single-sided joints in tension.

Key words: adhesive bonding, patch repairs, analytic model, nonlinear finite element analysis.

1. INTRODUCTION

During the last decades adhesive bonding has been widely used to construct and repair advanced structures, especially in the aircraft and automotive fabrication. The main advantage is the possibility to join parts from dissimilar materials as polymers, polymeric composites, aluminium, magnesium or other metal alloys. Bonded structures have been shown to be far more fatigue resistant than equivalent mechanically fastened structures. They are also low-priced and lighter due to the absence of fasteners, and more easily inspected by using non-destructive techniques.

The mechanical strength of adhesive bonded joint is strongly dependent on the adhesive properties, but the configuration of the joint and the bonding technique are also important. Correct evaluation of the in service behaviour of adhesively bonded joints is necessary to ensure the efficiency, safety and reliability of this kind of assembling [1].

While several joint geometries, such as the single- and double-lap joints have gained considerable attention, the single-strap configuration has received little consideration because earlier studies have shown it to be less efficient. However, many recent papers [2–10] have demonstrated that properly designed single-strap joints can be more efficient as single-lap joints.

University "Politehnica" of Bucharest, Romania

Rev. Roum. Sci. Techn. – Méc. Appl., Tome 55, Nº 3, P. 255–266, Bucarest, 2010

On the other hand, a good solution as the double-strapped joint is not applicable if the external surface of the structure is required to be smooth or if the access is only available from one side. Consequently, in many aircraft, automotive and other repair the only practical joint configuration is the single-strap joint. Usually, to repair a locally damaged structure, the patch is used to bridge a crack or to cover over a hole.

One of the objectives of paper [7] was to deny the statement that a single strapped joint is less efficient than the single-lap joint. This task was accomplished through a detailed analytical and numerical investigation of the joint parameters that govern the peak stresses in the adhesive.

If the outer adherends and the inner adherend (strap or patch) have the same tensile and bending stiffness, the joint is so-called balanced. In paper [7] the deformations of a typical unbalanced single-strapped joint were determined analytically and subsequently used to calculate the bending moments and the shear forces at the two ends of the overlap, that affect the peak stresses in the adhesive. In the case of a balanced single-strapped joint, closed-form solutions were obtained, but for an unbalanced joint the two differential equations are coupled and the solution can only be obtained numerically.

2. THE NONLINEAR ANALYTICAL CALCULUS

In practical engineering design, simple and accurate analytical solutions are very useful because they can provide a relatively fast preliminary estimation of the structural performances. Subsequent finite element analyses or experimental investigations are not always necessary.

A pre-dimensioning algorithm will be presented by using the calculus relations deduced in paper [7] for balanced single-strap joints with thin adhesive layer. The relations from the cited paper will be rewritten in a more convenient form for the design purposes. Two configurations of single-sided adhesive bonded repairs, with adherends of constant thickness (Fig. 1a) and with tapered adherends (Fig. 1b) will be analysed based on the same calculus scheme (Fig. 1c). A preliminary evaluation of the load capacity P (axial load per unit width) can be made as to accomplish the strength conditions in some locations of the joint. Allowable values are required for: a) combined tensile and bending maximum stress in the outer adherend, near the outer end of the overlap (zone 1), b) combined tensile and bending maximum stress in the inner adherend (strap), at middle and near the inner end of the overlap (zone 3), c) maximum equivalent stresses in adhesive (zone 2), at the adhesive layer ends.

The geometry that was considered (Fig. 1a) permits to analyse cases when the overlap (L_2) and the gap ($2L_3$) are small, mean or large. Fig. 2 shows the typical deformed shape in the case of a single-strapped joint. Because the dependence between the applied load and the stress state in the joint is nonlinear, to establish the allowed load will be a relatively difficult task. Due to symmetry, the discussion

that follows is referring to a half of the single-strapped joint, on which local axes were considered for each zone (Fig. 1c).

In the mentioned work [7], concerning the balanced single-strapped joints, the adherends were considered as cylindrically bended plates with bending stiffnesses:

$$D_k = \frac{E h_k^3}{12(1-\nu^2)} \qquad (k = 1, 2, 3), \tag{1}$$

where $h_1 = h_3 = h$ is the thickness of adherends which are made from the same material having the elastic modulus E and the Poisson's ratio ν.

The adhesive layer has a very small thickness h_a ($h_a << h$). Based on the assumption that the overlap (zone 2) works as a monobloc part, the thickness h_2 (Fig. 1c) will be considered as $h_2 = h_1 + h_3 + h_a$ in case of variant with right adherends (Fig. 1a), and as $h_2 = h_1 + h_4 + h_a$ when the adherends ends are tapered (Fig. 1b).

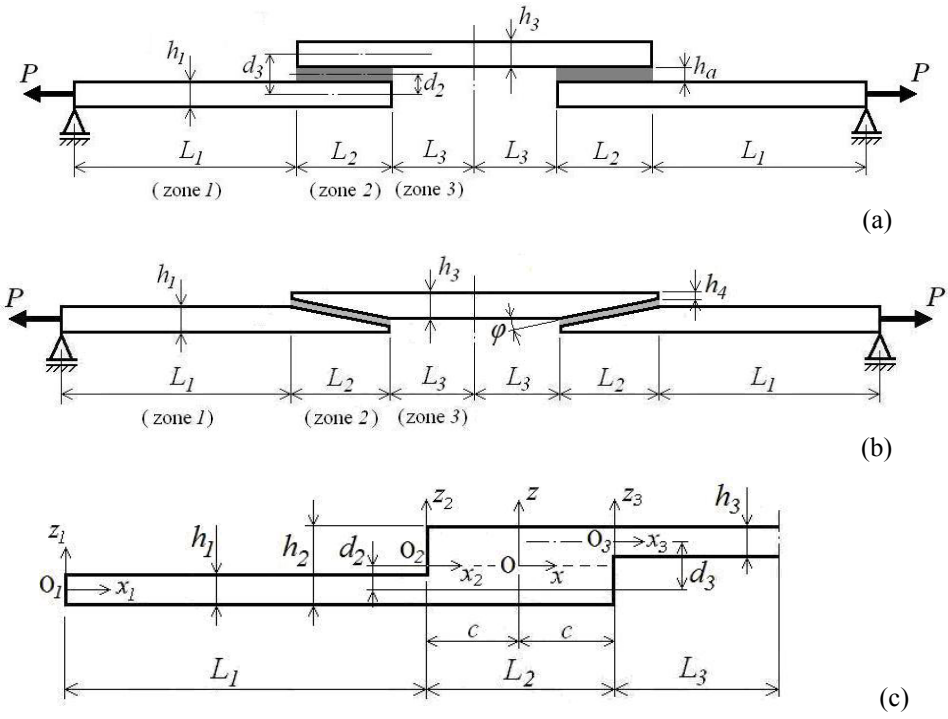

Fig. 1 – Geometries of single strapped joints: a) with right adherends; b) with tapered adherends; c) the simplified calculus scheme.

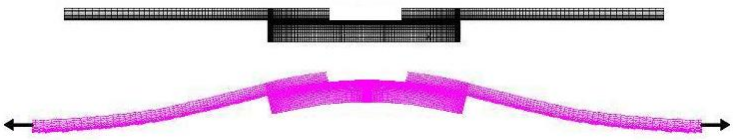

Fig. 2 – Deformed shape in case of a single-strapped joint.

The differential equations of the middle deformed surfaces of zones 1, 2 and 3 are

$$M_k = -D_k \frac{\mathrm{d}^2 w_k}{\mathrm{d}x_k^2} = -P\left(w_k + \mathrm{d}_k\right) \qquad \left(0 \le x_k \le L_k, \quad k = 1,\ 2,\ 3\right), \tag{2}$$

where M_k is the bending moment in region k of the joint, and d_k is the distance between the middle planes of zones 1 and k (k = 1, 2, 3). For clarity it is to note that $d_1 = 0$, that d_2 is measured between the middle planes of outer adherend and of adhesive layer, and d_3 is considered as the distance between the middle surfaces of outer and inner adherends (Fig. 1c).

The solution of differential equation (2) rewritten as

$$\frac{\mathrm{d}^2 w_k}{\mathrm{d}x_k^2} - \beta_k^2\left(w_k + \mathrm{d}_k\right) = 0, \qquad \text{with} \quad \beta_k = \sqrt{\frac{P}{D_k}}, \tag{3}$$

has the general form

$$w_k(x_k) = A_k \cosh(\beta_k x_k) + B_k \sinh(\beta_k x_k) + d_k, \quad (k = 1,\ 2,\ 3). \tag{4}$$

From proper boundary and continuity conditions, *i.e.*

$$w_1(0) = 0, \qquad w_1(L_1) = w_2(0), \qquad \left.\frac{\mathrm{d}w_1}{\mathrm{d}x_1}\right|_{x_1 = L_1} = \left.\frac{\mathrm{d}w_2}{\mathrm{d}x_2}\right|_{x_2 = 0}, \tag{5}$$

$$w_2(L_2) = w_3(0), \qquad \left.\frac{\mathrm{d}w_2}{\mathrm{d}x_2}\right|_{x_2 = L_2} = \left.\frac{\mathrm{d}w_3}{\mathrm{d}x_3}\right|_{x_3 = 0}, \qquad \left.\frac{\mathrm{d}w_3}{\mathrm{d}x_3}\right|_{x_3 = L_3} = 0, \tag{6}$$

were obtained the following expressions of the six integration constants:

$$A_1 = 0; \qquad B_1 = \frac{1}{N_3 \cosh(\beta_1 L_1)}\left[N_1 + d_2\left(\frac{\beta_2}{\beta_1}\tanh(\beta_2 L_2) + \frac{\beta_3}{\beta_1}\tanh(\beta_3 L_3)\right)\right], \tag{7}$$

$$A_2 = \frac{1}{N_3} \cdot \left[N_1 \cdot \tanh(\beta_1 L_1) - d_2\left(1 + \frac{\beta_3}{\beta_2} \cdot \tanh(\beta_2 L_2) \cdot \tanh(\beta_3 L_3)\right)\right], \tag{8}$$

$$B_2 = \frac{1}{N_3} \cdot \left[\frac{\beta_1}{\beta_2} \cdot N_1 + d_2 \left(\tanh(\beta_2 L_2) + \frac{\beta_3}{\beta_2} \cdot \tanh(\beta_3 L_3) \right) \right], \tag{9}$$

$$A_3 = -\frac{1}{N_3} \cdot \left[(d_3 - d_2) \cdot N_2 + \frac{\mathrm{d}_2}{\cosh(\beta_2 L_2)} \right]; \qquad B_3 = -A_3 \tanh(\beta_3 L_3), \tag{10}$$

where

$$N_1 = \frac{\beta_3}{\beta_1} \cdot \frac{\tanh(\beta_3 L_3)}{\cosh(\beta_2 L_2)} \cdot (d_3 - d_2), \tag{11}$$

$$N_2 = 1 + \frac{\beta_2}{\beta_1} \cdot \tanh(\beta_1 L_1) \cdot \tanh(\beta_2 L_2), \tag{12}$$

$$N_3 = N_2 + \beta_3 \cdot \tanh(\beta_3 L_3) \cdot \left(\frac{\tanh(\beta_1 L_1)}{\beta_1} + \frac{\tanh(\beta_2 L_2)}{\beta_2} \right). \tag{13}$$

The main purpose of developing an analytical solution was not the prediction of the lateral displacements of the joint, but the evaluation of the bending moments and shear forces at the inner and outer ends of the overlap (M_i, V_i and M_o, V_o). Their expressions, in a condensed form, are

$$M_i = D_3 \cdot \left. \frac{\mathrm{d}^2 w_3}{\mathrm{d} x_3^2} \right|_{x_3 = 0} = P A_3, \qquad M_o = D_1 \cdot \left. \frac{\mathrm{d}^2 w_1}{\mathrm{d} x_1^2} \right|_{x_1 = L_1} = P B_1 \sinh(\beta_1 L_1), \tag{14}$$

$$V_i = D_3 \cdot \left. \frac{\mathrm{d}^3 w_3}{\mathrm{d} x_3^3} \right|_{x_3 = 0} = \beta_3 P B_3, \qquad V_\mathrm{o} = D_1 \cdot \left. \frac{\mathrm{d}^3 w_1}{\mathrm{d} x_1^3} \right|_{x_1 = L_1} = \beta_1 P B_1 \cosh(\beta_1 L_1). \tag{15}$$

The distribution of the shear and peel stresses (τ and σ) in the adhesive, along the overlap (where $-c \le x \le c$ and $c = L_2/2$), can be estimated by using the expressions [5, 7]

$$\tau = C_0 + C_1 \cosh(\lambda x) + C_2 \sinh(\lambda x), \tag{16}$$

$$\begin{aligned} \sigma = {} & C_3 \cosh(\xi x) \cos(\xi x) + C_4 \cosh(\xi x) \sin(\xi x) + \\ & + C_5 \sinh(\xi x) \cos(\xi x) + C_6 \sinh(\xi x) \sin(\xi x), \end{aligned} \tag{17}$$

where

$$\lambda = \sqrt{\frac{G_a}{h_a}\cdot\left(\frac{2}{E\,h}+\frac{h(h+h_a)}{2D}\right)}; \qquad \xi = \sqrt[4]{\frac{E_a}{2\,h_a\,D}}, \tag{18}$$

as E_a, G_a are the tensile and the shear modules of the adhesive and $D = D_1 = D_3$.

The values of constants C_i (i = 0, 1, …, 6) will be calculated by the following formulas

$$C_0 = \frac{P}{2c} - \frac{G_a}{2c\lambda^2 h_a}\cdot\left[\frac{2P}{Eh}+\frac{h}{2D}\cdot\left(M_o - M_i\right)\right], \tag{19}$$

$$C_1 = \frac{G_a}{\lambda h_a \sinh(\lambda c)}\cdot\left[\frac{P}{Eh}+\frac{h}{4D}\cdot\left(M_o - M_i\right)\right], \tag{20}$$

$$C_2 = -\frac{G_a}{\lambda h_a \cosh(\lambda c)}\cdot\frac{h}{4D}\left(M_o + M_i\right), \tag{21}$$

$$C_3 = \frac{E_a}{4D\,h_a\,N_4}\left[\xi\left(H_{SC}-H_{CS}\right)\left(M_o - M_i\right)+H_{CC}\left(V_o + V_i\right)\right], \tag{22}$$

$$C_4 = \frac{E_a}{4D\,h_a\,N_5}\left[\xi\left(H_{CC}+H_{SS}\right)\left(M_o + M_i\right)+H_{CS}\left(V_o - V_i\right)\right], \tag{23}$$

$$C_5 = \frac{E_a}{4D\,h_a\,N_5}\left[\xi\left(H_{CC}-H_{SS}\right)\left(M_o + M_i\right)+H_{SC}\left(V_o - V_i\right)\right], \tag{24}$$

$$C_6 = \frac{E_a}{4D\,h_a\,N_4}\left[\xi\left(H_{SC}+H_{CS}\right)\left(M_o - M_i\right)+H_{SS}\left(V_o + V_i\right)\right], \tag{25}$$

where

$$N_4 = \xi^3\left(\cos(\xi c)\sin(\xi c)+\cosh(\xi c)\sinh(\xi c)\right), \tag{26}$$

$$N_5 = \xi^3\left(\cos(\xi c)\sin(\xi c)-\cosh(\xi c)\sinh(\xi c)\right), \tag{27}$$

$$H_{CC} = \cosh(\xi c)\cos(\xi c), \qquad H_{SS} = \sinh(\xi c)\sin(\xi c), \tag{28}$$

$$H_{CS} = \cosh(\xi c)\sin(\xi c), \qquad H_{SC} = \sinh(\xi c)\cos(\xi c). \tag{29}$$

Starting from the values of shear and peel stresses in the critical point of the adhesive, an equivalent stress can be calculated based on the von Mises's criterion

$$\sigma_{eq} = \sqrt{\sigma^2 + 3\tau^2} \,. \tag{30}$$

Following the design guide [11], the Hill's failure criterion will be applied to determine the maximum load that does not induces damages in the adhesive. The actual stress state is allowable in a point of the adhesive layer if the condition

$$\chi = \left(\frac{\sigma}{\sigma_{fa}}\right)^2 + \left(\frac{\tau}{\tau_{fa}}\right)^2 \le 1 \tag{31}$$

is accomplished, where σ_{fa} and τ_{fa} are the tensile and shear ultimate strengths of the adhesive. Also, the strength condition for the adherends (zones 1 and 3) can be written as

$$\sigma_{\max,ad} = \max\left(\sigma_{\max,\mathrm{I}}, \sigma_{\max,\mathrm{III}}\right) \le \sigma_a \,, \tag{32}$$

where

$$\sigma_{\max,I} = \frac{P}{h} + \frac{6M_{\mathrm{o}}}{h^2}; \qquad \sigma_{\max,\mathrm{III}} = \frac{P}{h} + \frac{6\left|M_i\right|}{h^2}, \tag{33}$$

and σ_a is the allowable stress in the material of the adherends.

If the gap at the adherends ends is small ($L_3 < h/2$), significant discrepancies will be registered between the results, because the analytical formulas become inaccurate. Especially, the value of the bending moment at the inner end of the overlap (M_i) and the maximum stresses in the adhesive are affected [7].

In the case of tapered adherends (Fig. 1b) it is to make a correction into relations (22)–(25), *i.e.* the binomials $(V_0 \pm V_i)$ must be replaced with $(V_0 \pm V_i)\cos\varphi$. In fact, in the majority of practical cases $\varphi < 8°$, and the correction is not necessary because $\cos\varphi \approx 1$.

3. COMPARISON BETWEEN THE STRESS STATES IN SINGLE STRAPPED JOINT WITH RIGHT AND TAPERED ADHERENDS

Results obtained by using the above presented relations will be compared with numerical ones, established by linear and nonlinear finite element analyses (NFEAs). The numerical results which will be discussed in this section were obtained by NFEAs performed by using COSMOS/M Finite Element System [12].

Each nonlinear analysis was developed by applying the load in 100 steps. If the final loading is too great and induces stresses of unacceptable values in adhesive and/or in the adherends, it is possible to identify the load capacity of the joint in a relatively simple manner: the load capacity is the maximum force which corresponds to a loading step where all strength conditions are accomplished.

Plane strain state and four node quadrilateral finite elements were used in the generation of numerical models. In order to validate the analytical model and to identify its limits of applicability, some numerical sets of joint geometric parameters were considered. In all cases was used the structural adhesive AV 119 (also known as Araldite® 2007) which has the following elastic and strength characteristics: $E_a = 3{,}000$ MPa, $\nu_a = 0.35$, $\sigma_{fa} = 70$ MPa, $\tau_{fa} = 47$ MPa. The shear modulus was deduced based on the assumption that the adhesive is an isotropic material, *i.e.* $G_a = 0.5 \cdot E_a / (1 + \nu_a) = 1{,}110$ MPa.

The first case which will be discussed is referring to a balanced single-strapped joint with right adherends (Fig. 1a) made from aluminium alloy having the elastic modulus E = 70,000 MPa, the Poisson's ratio $v = 0.33$ and the allowable stress $\sigma_a = 180$ MPa. The applied axial load (per unit width), $P = 145$ N/mm, induces a nominal tensile stress $\sigma_n = 50$ MPa into the adherends.

Dimensional parameters which were taken into account are: $L_1 = 80$ mm, $L_2 = 40$ mm, $L_3 = 10$ mm, $h = h_1 = h_3 = 2.9$ mm, $h_a = 0.2$ mm. The same main parameters were maintained for a joint with tapered adherends (Fig. 1b) and with $h_4 = 0.5$ mm. In these conditions, the above discussed correction is not necessary, because the tapering angle is small, $\varphi = \arctan\left[(h_3 - h_4)/L_2\right] = 3.43° < 8°$.

The values that are presented in Table 1 emphasize a good agreement between analytical and nonlinear elastic finite element analysis (NFEA) results.

Table 1

Comparison between analytical and numerical results

Variant	Calculus method	Maximum equivalent stresses in adherends [MPa]		Stresses at the inner ends of adhesive layers [MPa]			Maximum deflection [mm]
		Inner adherend	outer adherend	σ_{max}	τ_{max}	$\sigma_{eq,max}$	
right adherends	Analytic	237	113	58	38	87.7	1.37
	NFEA	240	135	59.7	39.5	90.8	1.54
	LFEA	395	114	111	66	159	5.46
tapered adherends	Analytic	88.7	67.3	12.0	16.8	31.5	0.342
	NFEA	91.1	72.0	13.5	14.6	28.7	0.376
	LFEA	130	69.6	20.3	21.3	42.1	1.77

The linear elastic finite element analysis (LFEA) predicts correctly only the maximum equivalent stress in the outer adherend. Consequently, this kind of joint must be evaluated based on nonlinear analytical and numerical models.

The main conclusion is that by tapering the adherends edges a spectacular reduction of maximum stresses in all components of the joint was obtained. In fact this is the effect of the reduction of the joint eccentricity (d_3) that is of 3.1 mm in case of right adherends and of 0.7 mm when the adherends are tapered.

The two variants, with right and tapered adherends will be compared based on results obtained by NFEAs. The diagrams from Fig. 3, that present the distribution of shear and peel stresses in the adhesive in the case of right adherends, emphasize a strong stress concentration at the inner ends of the overlaps and a less loaded portion (in the vicinity of the overlap middle).

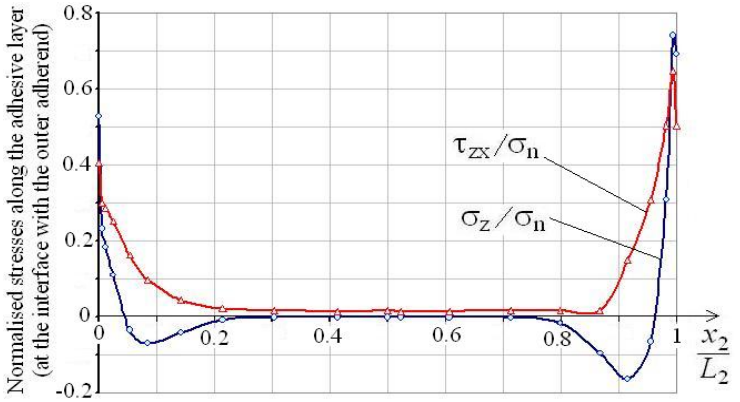

(a)

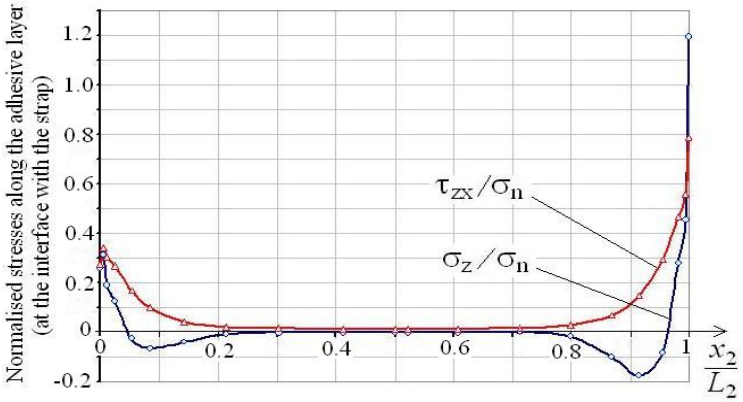

(b)

Fig. 3 – Distribution of shear and peel stresses along the adhesive layer in the case of a single-strapped joint with right adherends at the interface with: a) the outer adherend; b) the strap.

The stresses were normalised by dividing them with the nominal tensile stress in the outer adherends $\sigma_n = P/h_1 = 50$ MPa. The critical point in the adhesive is placed at the interface adhesive-strap at the inner ends of the overlaps where the maximum peel stress is 1.5 times greater than the maximum shear stress.

A completely different situation (Fig. 4) was observed in the case of the joint with tapered adherends where, in the critical point of the adhesive layer, the maximum shear stress is twice greater than the maximum peel stress. Because the stress distributions in the adhesive at the two interfaces are about the same, in Fig. 4 was presented only the variation of stresses along the interface with outer the adherend.

Based on results of NFEAs from Table 1, it is to observe that the maximum stress in adherends ($\sigma_{\max,ad}$) was reduced 2.63 times and the maximum equivalent stress in adhesive was reduced 3.16 times in the case of tapered adherends comparatively with the variant with right adherends.

In the case of the joint with right adherends the strength requirements (31) and (32) are not accomplished. On the contrary, the variant with tapered adherends is convenient, because $\chi = 0.133 < 1$ and $\sigma_{\max,ad} = 91.1 \text{ MPa} \le \sigma_a$.

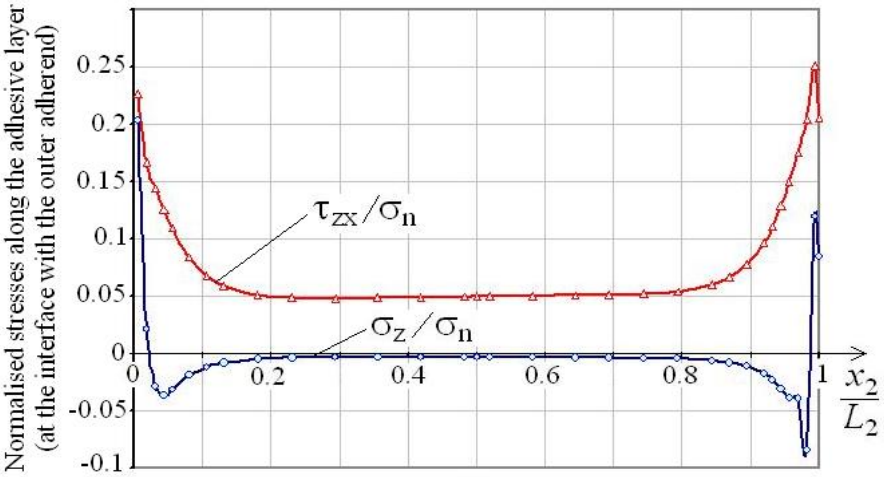

Fig. 4 – Distribution of shear and peel stresses along the adhesive layer in the case of a single-strapped joint with tapered adherends, at the interface with the outer adherend.

A study concerning the influence of the overlap length (L_2) was developed based on NFEAs for a repair with tapered adherends with the above presented main characteristics: $L_1 = 80$ mm, $L_3 = 10$ mm, $h = h_1 = h_3 = 2.9$ mm, $h_a = 0.2$ mm, $h_4 = 0.5$ mm. It is interesting to observe in table 2 that the overlap length has a relatively little influence on the stresses induced into the joint components.

Table 2

Influence of the overlap length (L_2) on the stress state in the joint with tapered adherends

L_2 [mm]	Maximum equivalent stresses in adherends [MPa]		Stresses at the inner ends of adhesive layers [MPa]			Maximum deflection [mm]
	Inner adherend	outer adherend	σ_{max}	τ_{max}	$\sigma_{eq,max}$	
20	97.4	72.1	22.9	19.4	40.7	0.307
30	94.1	72.1	16.9	16.5	33.1	0.345
40	91.1	72.0	13.5	14.6	28.6	0.376

4. **CONCLUSIONS**

The nonlinear analytical model is very useful for pre-dimensioning the balanced single-strapped adhesive bonded joints both in case of right or tapered adherends. A good agreement between analytical and nonlinear elastic finite element analysis results was observed. The linear elastic finite element analysis predicts correctly only the maximum equivalent stress in the outer adherend. Consequently, the behaviour of balanced or unbalanced single strapped joints, used to repair thin-walled damaged structures, will be evaluated correctly if nonlinear analytical or numerical models will be used.

For design purposes it is to underline that a spectacular improvement of the strength performances of single strapped-joints can be obtained by tapering the edges of the adherends and by using straps thicker than the outer adherends.

Received on July 26, 2010

REFERENCES

1. ADAMS, R.D., COMYN J., WAKE, W.C., *Structural adhesive joints in engineering,* London, Chapman & Hall, 1997.
2. DAVIES, M., BOND, D., *Principles and practice of adhesive bonded structural joints and repairs*, Int. Journal of Adhesion and Adhesives, **19**, pp. 91-105, 1999.
3. HART-SMITH, L.J., *Designing to minimize peel stresses in adhesive bonded joints*, in: *Delamination and debonding of materials* (Johnson W.S., editor), ASTM STP 876, pp. 238-266, 1985.
4. JARRY, E., SHENOI, R.A., *Performance of butt strap joints for marine applications*, Int. Journal of Adhesion and Adhesives, **26**, pp. 162-176, 2006.
5. LUO, O., TONG, L., *Closed-form solution for nonlinear analysis of single-sided bonded composite patch repairs*, AIAA Journal, **45**, *12*, pp. 2957-2965, 2007.
6. SANDU, M., SANDU, A., CONSTANTINESCU, D.M., SOROHAN St., *The effect of geometry and material properties on the load capacity of single-strapped adhesive bonded joints*, Key Engineering Materials, **339**, pp. 89-96, Trans Tech Publications, Switzerland, 2009.
7. SHAHIN, K., TAHERI, F., *Analysis of deformations and stresses in balanced and unbalanced adhesively bonded single-strap joints*, Composite Structures, **81**, pp. 511-524, 2007.

8. TAHERI, F., ZOU, G.P., *Treatment of unsymmetric adhesively bonded composite sandwich panels-to-flange joints,* Mechanics of Advanced Materials and Struct., **11**, pp. 175-196, 2004.
9. TONG, L., *Strength of adhesively bonded single-lap and lap-shear joints*, Int. Journal of Solid Structures, **35**, *20*, pp. 2601-2616, 1998.
10. WANG, C.H., ROSE L.R.F., *Determination of triaxial stresses in bonded joints*, I.J.A.A., **17**, pp. 17-25, 1997.
11. * * *, *Guide to the structural use of adhesives* (SETO), The Institution of Structural Engineers, London, 1999.
12. * * *, *COSMOS/M – Finite Element System*, *User Guide*, Structural Research & Analysis Corporation, USA, 1998.